Molecular Pharmacology Fast Forward. Published on June 30, 2014 as doi:10.1124/mol.114.094029
This article has not been copyedited and formatted. The final version may differ from this version.

Kinetic Organization of Ca^{2+} Signals that Regulate Synaptic Release Efficacy in Sympathetic Neurons

Michinori Mori, Shota Tanifuji and Sumiko Mochida

Department of Physiology, Tokyo Medical University, Tokyo 160-8402, Japan

Molecular Pharmacology Fast Forward. Published on June 30, 2014 as DOI: 10.1124/mol.114.094029
This article has not been copyedited and formatted. The final version may differ from this version.

Running title: **Kinetic Ca^{2+}phases control transmitter release**

***Corresponding author**: Sumiko Mochida, Department of Physiology, Tokyo Medical University, Tokyo 160-8402, Japan. E-mail: mochida@tokyo-med.ac.jp

Document statics

Number of text pages: 32
Number of figures: 5
Number of references: 50
Number of words in the abstract: 250
Number of words in the introduction: 498
Number of words in the discussion: 1394

Non-standard Abbreviation list

AP, action potential; AZ, active zone; BAPTA, 1,2-bis(2-aminophenoxy)ethane-N,N,N',N'-tetraacetic acid; BAPTA-AM, BAPTA-tetraacetoxymethyl ester; CaM, calmodulin; EGTA-AM, EGTA- tetraacetoxymethyl ester; EPSPs, excitatory postsynaptic potentials; ISIs, inter-stimulus intervals; PPD, paired-pulse depression; PPR, paired-pulse ratio; RP, reserve pool; RRP, readily releasable pool; RRSVs, release ready SVs; SCG, superior cervical ganglion; SVs, synaptic vesicles

Molecular Pharmacology Fast Forward. Published on June 30, 2014 as DOI: 10.1124/mol.114.094029
This article has not been copyedited and formatted. The final version may differ from this version.

Abstract

Calcium regulation of neurotransmitter release is essential for maintenance of synaptic transmission. However, the temporal and spatial organization of Ca^{2+} dynamics that regulate synaptic vesicle (SV) release efficacy in sympathetic neurons is poorly understood. Here, we investigate the N-type Ca^{2+} channels-mediated kinetic structure of Ca^{2+} regulation of cholinergic transmission of sympathetic neurons. We measured the effect of Ca^{2+} chelation with fast 1,2-bis(2-aminophenoxy) ethane-tetraacetic acid (BAPTA) and slow ethyleneglycol-tetraacetic acid (EGTA) buffers on exocytosis, synaptic depression, and recovery of the readily releasable vesicle pool (RRP), after both single action potential (AP) and repetitive APs. Surprisingly, postsynaptic potentials peaking at ~12 ms after the AP was inhibited by both rapid and slow Ca^{2+} buffers, suggesting that, in addition to the well-known fast Ca^{2+} signals at the active zone (AZ), slow Ca^{2+} signals at the peak of Ca^{2+} entry also contribute to paired-pulse or repetitive APs responses. Following single AP, discrete Ca^{2+}-transient regulated synaptic depression in a rapid (<30 ms) and slow (<120 ms) phase. In contrast, following prolonged APs trains, synaptic depression was reduced by a slow Ca^{2+} signal regulation lasting >200 ms. Finally, after an AP burst, recovery of the RRP was mediated by an AP-dependent rapid Ca^{2+} signal, and the expansion of releasable SV number by an AP firing activity-dependent slow Ca^{2+} signal. These data indicate that local Ca^{2+} signals operating near Ca^{2+} sources in the AZ are organized into discrete fast and slow temporal phases that remodel exocytosis and short-term plasticity to ensure long-term stability in acetylcholine release efficacy.

Molecular Pharmacology Fast Forward. Published on June 30, 2014 as DOI: 10.1124/mol.114.094029
This article has not been copyedited and formatted. The final version may differ from this version.

Introduction

Calcium ions are essential messengers that regulate various cellular processes. At the neuronal presynaptic active zone, an action potential (AP) results in opening of calcium channels and transient increases in Ca^{2+} of up to 200 μM at domains around the channel pore (Silver et al., 1994). Calcium channels are linked to synaptic vesicles (SVs) through SNARE proteins and a Ca^{2+}-sensing protein synaptotagmin that initiates SV exocytosis (Catterall, 2000). The distance between presynaptic Ca^{2+} channels and synaptotagmin determines the efficacy and speed of exocytosis, suggesting that the spatial diffusion of Ca^{2+} is crucial for the regulation of synaptic transmission (Neher and Sakaba, 2008, Eggermann et al., 2012). Likewise, it is known that other post-exocytosis Ca^{2+} receptors in presynaptic terminals control other aspects of synaptic function such as short-term plasticity (Catterall and Few, 2008, Catterall et al., 2013), replenishment of the readily releasable pool (RRP) (Llinás et al., 1991), SV endocytosis (Poskanzer et al., 2003, Nicholson-Tomishima and Ryan, 2004), and structural remodeling of presynaptic morphology (Su et al., 2012).

Following an AP, the spatial and temporal relationship between the Ca^{2+} source and Ca^{2+} sensors for various presynaptic functions can be probed using Ca^{2+} chelators with different Ca^{2+}-binding on-rates (*k*on), but comparable affinities (*K*D) (Adler et al., 1991); thus, 1,2-bis(2-aminophenoxy) ethane-tetraacetic acid (BAPTA) and ethyleneglycol-tetraacetic acid (EGTA) are ideal experimental tools for probing the kinetic organization of calcium signals because they differ by a factor of ~40 in their on-rates but have comparable substrate affinities (Naraghi, 1997, Naraghi and Neher, 1997, Nagerl et al., 2000). Thus, measurements of effects of BAPTA and EGTA on synaptic transmission can provide precise information about the distance between Ca^{2+}

Molecular Pharmacology Fast Forward. Published on June 30, 2014 as DOI: 10.1124/mol.114.094029
This article has not been copyedited and formatted. The final version may differ from this version.

channels and Ca^{2+} sensors (Cummings et al., 1996, Eggermann et al., 2012). For example, chelation data have been used to distinguish synaptic functions linked to Ca^{2+} signaling from nanodomain to microdomain coupling (Adler et al., 1991, Augustine et al., 1991, Tymianski et al., 1994, Cummings et al., 1996, Dittman and Regehr, 1998, Angleson and Betz, 2001).

Like exocytosis, presynaptic short-term plasticity and maintenance of the readily releasable pool (RRP) are regulated in a Ca^{2+} dependent-manner (Sakaba and Neher, 2001, Junge et al., 2004). After an AP, Ca^{2+} levels rapidly peak at the AZ and then gradually decline to resting levels. During this replenishment period various Ca^{2+} binding proteins act cooperatively to regulate SV competence to respond to incoming nerve signals (Mochida, 2011). However, the kinetic organization of these processes and their significance for the maintenance of various synaptic functions is largely unknown. In this study, we used Ca^{2+} chelators to examine the temporal regulation of the SV cycle by Ca^{2+} following AP firing in a model system for fast cholinergic transmission between rat superior cervical ganglion (SCG) neurons mediated by N-type Ca^{2+} channels activation (Mochida et al., 1996, Mochida et al., 2003). Collectively, the findings show that Ca^{2+} signals operating in and near AZs are organized into fast and slow temporal phases that trigger exocytosis and control short-term plasticity to ensure stability in SV release efficacy.

Materials and Methods

Ethical Approval

The Ethics Committee of Tokyo Medical University approved this project.

Molecular Pharmacology Fast Forward. Published on June 30, 2014 as DOI: 10.1124/mol.114.094029
This article has not been copyedited and formatted. The final version may differ from this version.

Culture of SCG neurons

Postnatal day 7 Wistar ST rats were decapitated under diethyl ether anesthesia according to the Guidelines of the Physiological Society of Japan. Isolated SCG neurons were maintained in culture as described previously (Mochida et al., 1994, Mochida et al., 1995, Ma and Mochida, 2007).

Electrophysiology

Synaptic transmission between SCG neurons. SCG neurons 5-9 weeks in culture were studied. Neurons were superfused with a modified Krebs solution consisting of 136 mM NaCl, 5.9 mM KCl, 2.5 mM $CaCl_2$, 1.2 mM $MgCl_2$, 11 mM glucose, and 3 mM Na-HEPES (pH 7.4, 23-25°C) (Lu et al., 2009). Presynaptic APs were generated by passing current through a sharp recording electrode filled with 1 M K-acetate (70–110 MΩ), and excitatory post synaptic potentials (EPSPs) were recorded from a neighboring neuron using another sharp electrode in all measurements of synaptic transmission.

Recording of ACh response. ACh responses were elicited in a postsynaptic neuron confirmed synaptic coupling with paired EPSP recording. ACh (Daiichi Sankyo Co. Ltd., Tokyo) at 100 μM was N_2 pressure-applied (5 psi for 1 s) through a puffer pipette at 0.1 Hz.

BAPTA-AM and EGTA-AM application. After a series of control EPSP or ACh response recordings, BAPTA-AM (Sigma-Aldrich Japan, Tokyo) or EGTA-AM (Life Technologies Corp. Japan, Tokyo) was bath-applied, at a final concentration of 50 μM or 1 μM (Fig. 2-5). 20 min later, another series of EPSP or ACh responses were

Molecular Pharmacology Fast Forward. Published on June 30, 2014 as DOI: 10.1124/mol.114.094029
This article has not been copyedited and formatted. The final version may differ from this version.

recorded. Data were collected using Clampex 10.2 (Molecular Devices, Downtown, PA). In Fig. 1, after stable EPSP recording for more than 20 min, chelators were bath-applied at a final concentration of 10, 50 or 100 μM for BAPTA-AM, or 1, 10, 50 or 100 μM for EGTA-AM. For bath-application, 15 μl of 0.1-10 mM chelators dissolved in 0.25-25% DMSO (Sigma-Aldrich Japan, Tokyo) was drop-applied to a 1.5 ml bath producing final concentrations of 1-100 μM (DMSO 0.0025-0.25%). As a control for 50 μM chelator carrier solution, 15 μl of 12.5% DMSO was drop-applied at a final concentration of 0.125%.

Analysis of EPSPs with various AP firing patterns

Data were analyzed with Origin software (Origin-Lab, Northampton, MA).

Paired-pulse ratio. To examine the rapid Ca^{2+} regulation of SVs in the RRP following AP generation, two consecutive APs at various inter-stimulus intervals (ISIs) were elicited in a presynaptic neuron every 1 min. Recordings for each ISI were performed in triplicate before and 20 min after bath-application of Ca^{2+} chelators. To calculate the paired-pulse ratio, the second EPSP amplitude measured from the end of the first EPSP was divided by the amplitude of the first EPSP measured from the base-line. The mean values of the paired-pulse ratio for individual synapse were calculated.

EPSPs with low-frequency AP trains. To examine Ca^{2+} regulation of SVs in the RRP in response to consecutive low-frequency AP firing, an AP was elicited in a presynaptic neuron at 0.1 Hz or 0.25 Hz. EPSP amplitudes were normalized to the mean EPSP amplitudes from 10 min recording before bath application of Ca^{2+} chelators. Normalized and averaged EPSP amplitudes were smoothed using 8 point adjacent averaging in Origin 8. To compare the rate of EPSP reduction, the normalized values were fitted with

Molecular Pharmacology Fast Forward. Published on June 30, 2014 as DOI: 10.1124/mol.114.094029
This article has not been copyedited and formatted. The final version may differ from this version.

exponential curves.

EPSPs with high-frequency AP trains and estimation of the RRP size. To examine Ca^{2+} regulation of SVs in the RRP in response to consecutive high-frequency AP firing, 2-s AP trains at 5, 10, or 20 Hz were elicited. For each frequency, AP trains were performed in triplicate every 2 min before and 20 min after bath application of Ca^{2+} chelators. To compare changes in SVs in the RRP during 2-s trains, the peak amplitude measured from the base-line was normalized to the first EPSP amplitude. The RRP size was estimated from back-extrapolation (to time=0) of average cumulative EPSP amplitudes recorded at 20 Hz (Schneggenburger et al., 1999) using Origin 8. Number of synaptic vesicles in the RRP was estimated by dividing the value of the RRP size with the mean value of the quantal EPSP amplitude (0.4 mV)(Krapivinsky et al., 2006)

RRP depletion and recovery. After a 1-min control EPSP recording at 1 Hz, a 3- or 4-min AP trains at 5 Hz were applied to deplete SVs in the RRP, and then EPSPs were recorded at 1 Hz. A series of recording was performed before and 20 min after application of Ca^{2+} chelators. EPSP amplitudes were normalized to the mean EPSP amplitudes before the AP trains using Origin 8. Averaged EPSP amplitudes were smoothed using Origin 8 as described above.

Time constant for RRP recovery. Averaged EPSP amplitudes after 4-min AP trains in control and in the presence of Ca^{2+} chelators or DMSO were fitted with single exponential growth curves from 0 to 2 s or from 1 to 6 min using Origin 8. To show clearly the fast recovery rate, the mean value of base-line noise level recording at time=0 (< 1 mV), was subtracted from mean EPSP amplitudes (Tanifuji et al., 2013).

Short-term Plasticity. Two forms of presynaptic short-term enhancement of synaptic transmission, termed augmentation and post-tetanic potentiation (PTP) were elicited by

Molecular Pharmacology Fast Forward. Published on June 30, 2014 as DOI: 10.1124/mol.114.094029
This article has not been copyedited and formatted. The final version may differ from this version.

10-s AP trains at 20 Hz or 60-s AP trains at 40 Hz (Mochida et al., 2008). After 3-min control EPSP recording at 1 Hz, AP trains were applied, and then EPSPs were recorded at 1 Hz. A series of recording was performed before and 20 min after bath-application of Ca^{2+} chelators. Mean EPSP amplitudes measured 1 min after the AP train was expressed as a percentage of mean EPSP amplitude from 1 min control recording before application of AP trains.

Statistics

Statistical significance was determined by two-tailed Student's *t* test, nonparameric Mann Whitney U-test or one-way ANOVA. All data are shown as the mean plus/minus S.E.M. Statistical significance was assumed when $p<0.05$, $p<0.03$, $p<0.01$, or $p<0.001$.

Results

BAPTA and EGTA reduce release probability

BAPTA has rapid-on-rate Ca^{2+} chelating properties which are useful for studying Ca^{2+} regulation of synaptic functions in close proximity to the Ca^{2+} source (e.g. the voltage-gated Ca^{2+} channel pore) (Eggermann et al., 2012), while EGTA has slow-on-rate Ca^{2+} chelating properties useful for studying Ca^{2+} regulation of synaptic functions within more distant areas from the Ca^{2+} source. Given the constant rate of Ca^{2+} diffusion in cytoplasm, the temporal kinetics of Ca^{2+} signals can also be measured and compared to Ca^{2+}'s spatial range. Thus, EGTA and BAPTA have been used to study the spatial and temporal Ca^{2+} regulation of neurotransmission (Adler et al., 1991, Augustine et al., 1991, Tymianski et al., 1994, Cummings et al., 1996, Dittman and Regehr, 1998, Angleson and Betz, 2001). In this study, using these chelators, we

Molecular Pharmacology Fast Forward. Published on June 30, 2014 as DOI: 10.1124/mol.114.094029
This article has not been copyedited and formatted. The final version may differ from this version.

examined the kinetic organization of SV ability at the AZ for either low or high frequency AP signals in synaptically-coupled SCG neurons (Mochida et al., 1994).

We first examined the efficacy of membrane-permeable Ca^{2+} chelators, monitoring cholinergic synaptic transmission by applying low frequency presynaptic APs at 0.1 Hz during their bath application. 10 μM BAPTA-AM showed no effect on synaptic transmission, however, 50 or 100 μM BAPTA-AM, rapidly, and then gradually, decreased excitatory postsynaptic potential (EPSP) amplitude over a 40 min recording period (Fig. 1A, B). The EPSP amplitude reduction was dose-dependent. A 0.5% DMSO control had no significant effect on EPSP amplitude (n=5, 8; Fig. 1B, C). In contrast, EGTA reduced EPSP amplitude more effectively than BAPTA (Fig. 1E, F). 10, 50, and 100 μM EGTA-AM showed a similar maximum effect on EPSP amplitude reduction (Fig. 1F). The EGTA-AM effect appeared shorter than the BAPTA-AM effect, suggesting that permeability of the chelators into the presynaptic terminal may be different. The rate of EPSP amplitude reduction was more rapid than that with BAPTA-AM (Fig. 1C, D, G, H). The time constant for the reduction of EPSP amplitude at 0.1 Hz, 2.2 ± 0.5 min (mean ± SEM, n=7), with 100 μM EGTA-AM was 4 fold faster than the time constant (9.1± 1.2 min, n=7) with 100 μM BAPTA-AM. The rate of EPSP amplitude reduction with EGTA was dose-dependent (Fig. 1H), but not SV-use-dependent (Fig. 1G, I), suggesting a reduction in the probability that a SV in the RRP will undergo fusion in response to a single AP (Pv).

Effect of Ca^{2+} chelators on basal Pv should be activity-independent. We tested this by treating with chelators in the absence of synaptic activity. The EPSP recording was stopped after 1 μM EGTA-AM or 50 μM BAPTA-AM was bath-applied (Fig. 1J, K) and re-started 20 min later. This later EPSP amplitude was ~60% of that before

Molecular Pharmacology Fast Forward. Published on June 30, 2014 as DOI: 10.1124/mol.114.094029
This article has not been copyedited and formatted. The final version may differ from this version.

EGTA-AM application and ~40% of that before BAPTA-AM application (Fig. 1L). The postsynaptic ACh response was not significantly reduced by BAPTA-AM (Fig. 1M) or EGTA-AM (Fig. 1N). Thus, both rapid- and slow-on-rate Ca^{2+} chelators reduced the presynaptic Pv, suggesting that both fast and slow local Ca^{2+} signals regulate release efficacy at the AZ during ongoing transmitter release.

The kinetics of transmitter release was altered by 1 μM EGTA-AM, but not significantly by 50 μM BAPTA-AM (Fig. 1A, E). BAPTA may chelate Ca^{2+} before reaching the maximal concentration at vesicle release sites, therefore the EPSP peak amplitude was reduced (Fig. 1Aa) but the time course was not altered (Fig. 1Ab). EPSP time-to-peak after an AP firing (12 ± 0.4 ms, n=5) was delayed 2.3 ± 0.4 ms after application of EGTA (mean of three averaged traces of 15-16, 25-26 and 35-36 min after EGTA application) (Fig. 1Eb). The EPSP decay was accelerated (control decay time constant 33 ±1.5 ms *vs*. 26 ± 1.2 ms after 1 μM EGTA application)(Fig. 1Ea). These results provide new insight showing that EGTA apparently affects the kinetics of the Ca^{2+} peak transient. Consistently, a Ca^{2+} imaging study in hippocampal neurons reported that a single AP-driven presynaptic Ca^{2+} signal peaked within 1 ms, half of which was chelated by EGTA-AM (Hoppa et al., 2012).

Ca^{2+} entry during low frequency firing regulates SV availability in the RRP

We examined the role of Ca^{2+} signals in determining SV competence to respond to an incoming AP by comparing the recovery kinetics of release ready SVs (RRSVs) during low frequency synaptic activity consisting of consecutive presynaptic APs at 0.1 and 0.25 Hz. The rate of EPSP reduction with EGTA-AM was dose-dependent (Fig. 1H), but not firing activity-dependent (Fig. 1G, I), suggesting a reduction of basal Pv. In

Molecular Pharmacology Fast Forward. Published on June 30, 2014 as DOI: 10.1124/mol.114.094029
This article has not been copyedited and formatted. The final version may differ from this version.

contrast, the rate of EPSP reduction with BAPTA-AM was firing activity-dependent. 20 min after 100 μM BAPTA-AM application, the EPSP amplitude decreased 57% for 0.1 Hz and 80% for 0.25 Hz AP firing (Fig. 1C). The time constant for the reduction of RRSVs at 0.25 Hz AP firing (4.1 ± 0.6 min, n=5) was ~half of that at 0.1 Hz (9.1 ± 1.7 min, n=6) (Fig. 1D). Unexpectedly, BAPTA reduced RRSVs in a SV-use-dependent manner, suggesting the presence of a rapid Ca^{2+} signal mediated regulation following each AP-driven Ca^{2+} entry during low frequency firing supports replenishment of the RRP.

Ca^{2+} entry following a single AP regulates SV availability in the RRP

Next, we examined the temporal Ca^{2+} signals underlying SV availability at the AZ following a single AP. Applying a paired-pulse protocol, we monitored SV release efficacy of the RRP following a single AP-driven Ca^{2+} transient. The amplitude of the first EPSP (inter-stimulus interval, ISI=15 ms) before BAPTA or EGTA application was 22.5 ± 2.1 mV (n=8) and 20.7 ± 2.7 mV (n=9), respectively (Fig. 2A). 20 min after 50 μM BAPTA-AM or 1 μM EGTA-AM application, the amplitude of the first EPSP was 7.0 ± 1.5 mV and 14.1 ± 2.2 mV, respectively (Fig. 2A). This represents a reduction of ~ 69% for BAPTA and ~32% for EGTA. As a control measurement, the amplitude of the first EPSP was similar for all ISI in the presence of chelators (Fig. 2B, C). These results suggest that both chelators reduce Pv, but induce no further changes in the first response of consecutive paired APs.

In control recordings before Ca^{2+} chelator application, paired-pulse depression (PPD) was observed (Fig. 2D, E). The amplitude of the second EPSP with an ISI of 15 ms increased in the presence of BAPTA (Fig. 2B), while it increased with ISIs of 15, 30

Molecular Pharmacology Fast Forward. Published on June 30, 2014 as DOI: 10.1124/mol.114.094029
This article has not been copyedited and formatted. The final version may differ from this version.

and 60 ms in the presence of EGTA (Fig. 2C). The paired-pulse ratio showed a reduction of PPD with an ISI < 30 ms with BAPTA (Fig. 2D). In contrast, EGTA reduced PPD with ISIs 30, 40, 60 and 120 ms (Fig., 2E). These results are consistent with EGTA having effects at longer ISI values than BAPTA, however, the time course for both agents is slower than that seen for chelating actions on Ca^{2+} transients shown above. These findings suggest that PPD may be mediated by a secondary process to Ca^{2+} transients, such as that involving a Ca^{2+}-sensor intermediate, e.g. calmodulin (CaM) that controls Ca^{2+} channel activity in SCG synapses (Mochida et al., 2008).

Ca^{2+} entry during high frequency AP firing regulates SV availability in the RRP

To further examine the relationship of temporal Ca^{2+} signal dependent regulation of SV ability for repetitive signal inputs, replenishment of RRSVs during repetitive firing was examined in the presence of Ca^{2+} chelators. 2-s AP trains at 5, 10 or 20 Hz were applied in triplicate every 2 min. We tested frequencies of AP firing within the physiological range for sympathetic neurons (Libet and Mochida, 1988), and avoided strong, non-physiological stimulation. AP trains at high frequencies of 5, 10 and 20 Hz induced synaptic depression (Fig. 3A and B, Control and DMSO). Synaptic depression was accelerated with higher firing rates. In the presence of 50 μM BAPTA-AM, the amplitude of the first EPSP reduced [EPSP reduction: 50 ± 3% (5 Hz), 42 ± 5% (10 Hz), 47 ± 4% (20 Hz), each normalized to the amplitude of the first EPSP before BAPTA-AM, n=5-6], however, the EPSP amplitudes following consecutive APs at 5 Hz were similar to that of control after the third EPSP (Fig. 3Ba), like the effect of BAPTA-AM for PPD with ISI of 200 ms (Fig. 2D). In contrast, in the presence of 1 μM EGTA-AM, the EPSP size from the first to the 10th with three different AP firing rates

Molecular Pharmacology Fast Forward. Published on June 30, 2014 as DOI: 10.1124/mol.114.094029
This article has not been copyedited and formatted. The final version may differ from this version.

were all smaller than that of before EGTA treatment (Fig. 3Ba-c), suggesting a slow Ca^{2+} signal mediated reduction of synaptic depression during AP trains at high frequencies. 2 min after cessation of each 5 or 10 Hz train, the amplitude of the first EPSP returned to the initial value with both chelators. These results suggest that a slow Ca^{2+} signal mediated regulation, lasting more than the 200 ms AP firing interval and completed within 2 min, is important for maintaining RRSVs in the RRP during high frequency AP firing.

The release efficacy in this series of recordings was reduced to 0.54 ± 0.04 with 50 μM BAPTA-AM and 0.55 ± 0.02 with 1 μM EGTA-AM, calculated from the mean amplitude of the first EPSP for 5, 10 and 20 Hz. In addition, the number of releasable SVs in the RRP [estimated from the back-extrapolation (to time=0) of cumulative EPSP amplitudes recorded at 20 Hz (Schneggenburger et al., 1999, Inchauspe et al., 2007)] (Fig. 3C) was significantly reduced with BAPTA or EGTA (43 or 48 SVs), in contrast to before the application of Ca^{2+} chelator (105 or 105 SVs) or DMSO (94 SVs) (BAPTA *vs.* before BAPTA, $p<0.001$; EGTA *vs.* before EGTA, $p<0.001$; before BAPTA *vs.* before EGTA, $p>0.05$; BAPTA *vs.* EGTA, Bonferroni post hoc test after one-way ANOVA). These results suggest that both rapid and slow Ca^{2+} signals regulate the RRP to maintain stable neurotransmitter release during high presynaptic firing activity. Alternatively, the effects of BAPTA and EGTA on apparent pool size could be explained by assuming that a decreased Pv leads to a smaller effective pool size (Leao and von Gersdorff, 2009, Thanawala and Regehr, 2013).

Ca^{2+} entry regulates SV pool recovery

We next investigated how rapid and slow Ca^{2+} signals contribute to SV recycling into

Molecular Pharmacology Fast Forward. Published on June 30, 2014 as DOI: 10.1124/mol.114.094029
This article has not been copyedited and formatted. The final version may differ from this version.

the RRP. The recovery of RRSVs following full depletion of the SV pool due to 4-min AP trains at 5 Hz was monitored by measuring the EPSP amplitude every 1 s. 5 min after a series of control recording, 50 μM BAPTA-AM or 1 μM EGTA-AM was bath-applied and, 20 min and 40 min later, two series of recordings with a 5 min interval were performed. As a control, cells were exposed to 0.5 % DMSO, at 20-21 min or 40-41 min the mean EPSP amplitude was 98.0 ± 1.4 % or 77.7 ± 1.3% of control before the AP train and DMSO application (n=7). The mean EPSP amplitude with BAPTA was 73.5 ± 1.1 % or 57.5 ± 1.1% of control (n=9), while it with EGTA was 77.4 ± 0.1 % or 52.6 ± 0.1% of control (n=11). These values, smaller in reduction of EPSP amplitude than that of above experiments, may reflect that we selected strong synapses for the SV pool recovery experiment. After 5 min interval of the EPSP recording, the release efficacy of SVs for the second recording with BAPTA and EGTA was 74% and 68% of control in the presence of DMSO. These results suggest that both rapid and slow Ca^{2+} signal mediated regulation underlie RRP replenishment.

We next analyzed the kinetics associated with Ca^{2+} entry in the activation of SV recycling pathways. Previously we showed that after depletion of the RRP, the SV pool recovers at two time constants, fast and slow, through dynamin-mediated distinct endocytosis pathways (Lu et al., 2009, Tanifuji et al., 2013). Here, to map Ca^{2+} specificity onto the fast and slow components, we compared recovery time constant with exponential growth curves fitted to the increase in the mean EPSP amplitude 2 s (during the fast recovery) and 1-6 min (during the slow recovery) after cessation of the AP train. Control recordings had a time constant for fast and slow recovery of τ=3.4 ± 0.5 s, 4.4 ± 0.3 min, respectively. Recovery rates of fast and slow phases were delayed by BAPTA (Fig. 4D and E). To obtain a clearer comparison of rapid Ca^{2+} signal

Molecular Pharmacology Fast Forward. Published on June 30, 2014 as DOI: 10.1124/mol.114.094029
This article has not been copyedited and formatted. The final version may differ from this version.

mediated regulation of RRP recovery, data was measured over 2 s after depletion of SVs (Fig. 4D). In contrast to BAPTA, EGTA showed a delay only in the slow rate of recovery (Fig. 4E). Thus, kinetic analysis suggests rapid and slow Ca^{2+} signals may regulate the specificity of fast and slow endocytosis pathways. In addition, these results suggest that slow Ca^{2+} signal regulation does not contribute to control of the rapid RRP replenishment rate, but does determines the RRP size through RP replenishment activated by a long train of AP firing (Lu et al., 2009, Tanifuji et al., 2013).

Ca^{2+} entry regulates SV availability for the short-term plasticity

At the presynaptic terminal, rapid responses to ongoing changes in AP firing are critical for short-term plasticity, which is important for encoding information in the nervous system (Abbott and Regehr, 2004). Augmentation and post-tetanic potentiation (PTP), which lasts for seconds to minutes, are thought to induce Ca^{2+} accumulation in response to short and longer AP trains (Zucker and Regehr, 2002). Therefore, we investigated how rapid and slow Ca^{2+} signals contribute to augmentation and PTP by applying a 10-s conditioning AP train at 20 Hz or a 60-s train at 40 Hz (Mochida et al., 2008). We selected smaller EPSPs (10 ± 0.9 mV, n=35) to avoid AP generation after the conditioning train.

1 μM EGTA-AM significantly reduced the magnitude of augmentation (Fig. 5A) and accelerated the decay rate (Fig. 5A, insert). The mean EPSP amplitude measured 1 min after a 10-s AP train at 20 Hz increased 2.2 fold, whereas the increase was 1.3 fold in the presence of EGTA (Fig. 5A). The enhancement with EGTA was 65 ± 5.4% of control (n=7), while it was 115 ± 8.4 % (n=5) with 50 μM BAPTA-AM or 96 ± 7.8% (n=4) with DMSO ($p<0.05$, BAPTA-AM *vs.* EGTA-AM Bonferroni post hoc

Molecular Pharmacology Fast Forward. Published on June 30, 2014 as DOI: 10.1124/mol.114.094029
This article has not been copyedited and formatted. The final version may differ from this version.

test after one-way ANOVA) (Fig. 5D). Thus, EGTA significantly reduced the magnitude of augmentation (Fig. 5A). In addition, EGTA accelerated the decay rate of augmentation from a control value τ=2.8 ± 0.3 min to τ=1.8 ± 0.2 min (n=7) ($p<0.05$, control *vs.* EGTA-AM, paired Student' s *t* test) (Fig. 5A, insert).

The mean EPSP amplitude measured 1 min after a 60-s AP train at 40 Hz increased 2.5 fold, whereas the increase was 2.3 fold in the presence of EGTA (Fig. 5F). In contrast, the increase was 2.7 fold before BAPTA application, and 1.7 fold in the presence of BAPTA (Fig. 5F). The enhancement with BAPTA was 64 ± 6.4% of control (n=7), while with EGTA or DMSO it was 96 ± 11.4 % (n=6) or 83 ± 14.7% (n=6), respectively ($p<0.05$, BAPTA-AM *vs.* EGTA-AM, Bonferroni post hoc test after one-way ANOVA) (Fig. 5H). Surprisingly, BAPTA, but not EGTA, significantly reduced PTP magnitude, but did not change the decay rate; τ=2.5 ± 0.4 min for control and τ=2.7 ± 0.4 min for BAPTA (n=7), respectively (Fig. 5F, insert). These results suggest that rapid and slow Ca^{2+} signals differentially contribute to the generation of short-term plasticity. Rapid Ca^{2+} signals partially mediate the generation of PTP and slow Ca^{2+} signals contribute to the generation and maintenance of augmentation.

Discussion

In this study we address how the time course of Ca^{2+} signaling at the release site regulates the ability of synaptic vesicles to respond to AP firing to maintain stable synaptic transmission. Our findings indicate that Ca^{2+} signals acting at both fast and slow time scales following a single or multiple AP have differential effects on exocytosis, releasable vesicle pool replenishment, and short-term plasticity that together ensure the long-term stability of SV release efficacy. Collectively, these findings

Molecular Pharmacology Fast Forward. Published on June 30, 2014 as DOI: 10.1124/mol.114.094029
This article has not been copyedited and formatted. The final version may differ from this version.

describe the kinetic organization of Ca^{2+} signals in presynaptic vesicle release.

Phasic Ca^{2+} signaling regulates release probability and short term plasticity

The release probability of SVs for exocytosis (Pv) *via* Ca^{2+} influx through AZ voltage-gated calcium channels shows a steep nonlinear Ca^{2+} dependence (Mochida et al., 2008). In hippocampal neurons, high concentrations of EGTA-AM reduced the peak Ca^{2+} transient and SV exocytosis induced by a single AP by approximately 50% (Hoppa et al., 2012). Our findings also suggest that EGTA, in addition to BAPTA, can reduce Pv in peripheral sympathetic neurons (Fig. 1-5). The EPSP peak of 12 ms after the AP was delayed 2.3 ms by EGTA, suggesting that EGTA chelates peak Ca^{2+} elevation in SCG neurons. Our results from EGTA application match the "domain overlap regimen," suggested by experiments showing that even slow buffers of the EGTA type at moderate concentrations are capable of reducing synaptic transmission of immature (Borst and Sakmann, 1996) but not mature calyx synapses (Yang et al., 2010) . Thus, rapid reduction of EPSPs with EGTA following presynaptic APs at 0.1 Hz (Fig. 1E, F) likely reflects reduction of phasic Ca^{2+} transients at the AZ, but not tonic residual Ca^{2+} from previous APs. Together, our results indicate that Pv is controlled spatially and temporally by Ca^{2+} transient increases chelated with fast and slow time-dependence by both BAPTA and EGTA.

A change in the paired-pulse ratio (PPR) could reflect either a basal change in Pv before stimulation or an activity-dependent change in Pv following stimulation. When PPRs are altered by changes in basal Pv before stimulation, the PPR is inversely proportional to the amplitude of the first EPSP (Zucker and Regehr, 2002). In our study, BAPTA or EGTA reduced the basal Pv and PPR with an ISI <30 ms or <120 ms,

Molecular Pharmacology Fast Forward. Published on June 30, 2014 as DOI: 10.1124/mol.114.094029
This article has not been copyedited and formatted. The final version may differ from this version.

respectively, suggesting phasic Ca^{2+} signal regulation of RRSVs in addition to Ca^{2+} control of the basal Pv. In SCG neurons, PPD with an ISI <120 ms is mediated by the Ca^{2+}-sensor protein CaM *via* its binding to the Ca^{2+} channel C-terminal domain (Mochida et al., 2008, Magupalli et al., 2013). The N-lobe of CaM rapidly binds Ca^{2+} within the Ca^{2+} channel nanodomain (Faas et al., 2011) and inhibits Ca^{2+} channel activity (Lee et al., 2003).

Phasic and tonic Ca^{2+} signaling underlie maintenance of the releasable pool of SVs

We observed that BAPTA reduced the releasable SV pool in a SV-use-dependent manner under relatively low presynaptic activity (Fig. 1), suggesting the existence of a novel low affinity Ca^{2+}-sensor in RRP replenishment. A candidate sensor may be the low affinity Ca^{2+} sensor isoform of synaptotagmin that may regulate endocytosis in *Drosophila* neuromuscular synapse and mammalian cortical synapses (Poskanzer et al., 2003, Nicholson-Tomishima and Ryan, 2004). The reduction of RRP was accelerated during repetitive AP firing at 0.25 Hz than at 0.1 Hz in the presence of BAPTA (Fig. 1), suggesting that this from of rapid Ca^{2+}-mediated regulation may last longer than 4 s. However, a rapid Ca^{2+}-mediated regulation of the releasable SV pool was not obvious during high frequency of AP firing at 5 Hz (Fig. 3), suggesting that a rapid Ca^{2+} signal mediated RRSV replenishment takes <200 ms after a single AP firing under higher presynaptic activity. It appears unlikely that resupply of RRSV *via* endocytosis can be completed <200 ms because the imaging studies show endocytosis occurring on a timescale of seconds (Poskanzer et al., 2003, Nicholson-Tomishima and Ryan, 2004). However, 'flash-and-freeze' approach revealed ultrafast mode of dynamin-mediated endocytosis which occurs within 50-100 ms after the AP (Watanabe et al., 2013). In

Molecular Pharmacology Fast Forward. Published on June 30, 2014 as DOI: 10.1124/mol.114.094029
This article has not been copyedited and formatted. The final version may differ from this version.

contrast to BAPTA, EGTA rapidly reduced the EPSP amplitude following a high frequency (at 5 Hz, 200 ms interval) AP train (Fig. 3), and within 2 min of train initiation the amplitude recovered to the initial value of the first EPSP. Thus, the time window for a slow Ca^{2+}-dependent regulation of RRSVs is >200 ms and <2 min (Fig. 3). This time scale suggests that SVs recycle *via* molecular sensors for endocytosis. Endocytosis at many synapses requires initiation by Ca^{2+}/CaM (Wu et al., 2009) and dynamin (Tanifuji et al., 2013) that mediates fission of SVs from the presynaptic terminal membrane (Takei et al., 1995). The precise Ca^{2+} triggering pathway for endocytosis is not well established but it known that dynamin activation by calcineurin is Ca^{2+}/CaM-dependent (Cousin and Robinson, 2001). In SCG neurons, dynamin 3 and 1 mediate endocytosis with fast and slow latency of their activation after an AP, respectively, while dynamin 2 mediates both modes of endocytosis (Tanifuji et al., 2013). Our present study demonstrates that two different forms of phasic and tonic Ca^{2+} signaling dependent RRP replenishment are generated by low and high AP firing activity, respectively. Ca^{2+}-sensors, mediators, and effectors for the activity-dependent and -independent endocytosis in SCG neurons are under examining.

Phasic and tonic Ca^{2+} signals control kinetics and magnitude of RRP replenishment following high frequency AP firing

Our results indicate that Ca^{2+} has an essential kinetic role in both rapid and slow changes in the RRP size, which can be defined as the number of SVs accessible for exocytosis in response to an AP (Rizzoli and Betz, 2005). Following RRP depletion with high frequency AP trains, both rapid and slow Ca^{2+}-dependent regulation mediate recovery with fast (τ<3.4 s) and slow (τ<4.4 min) kinetics (Fig. 4). We have shown

Molecular Pharmacology Fast Forward. Published on June 30, 2014 as DOI: 10.1124/mol.114.094029
This article has not been copyedited and formatted. The final version may differ from this version.

previously that the fast process corresponds to rapid RRP refilling with SVs from the RP in an amphiphysin- and dynamin 1, 2-dependent endocytic pathway, while the slow process involves a slow refilling of the RRP with SVs through an amphiphysin-independent and dynamin 2, 3-dependent endocytic pathway that bypasses the RP (Lu et al., 2009, Tanifuji et al., 2013). During and after high frequency firing, a reduction in the RRP size accelerate amphiphysin- and dynamin 1, 2-dependent endocytic pathway to refill the RP (Tanifuji et al., 2013), resulting in the recovery of the basal RRP.

Inhibition of the rapid Ca^{2+} signal with BAPTA slowed the rapid recovery rate (Fig. 4A, D), suggesting control of the SV kinetics in the RP pathway by an active zone protein which forms a protein network with other active zone proteins including Ca^{2+}-binding proteins, like activity-dependent RRP reloading controlled by Bassoon in central excitatory synapse (Hallermann et al., 2010). In contrast, loss of slow Ca^{2+} signal with EGTA reduced the magnitude of rapid recovery (Fig. 4B), suggesting direct control of RP size by tonic Ca^{2+} signaling to regulate slow endocytosis (Tanifuji et al., 2013) and/or SVs release from the RP into the RRP (Llinás et al., 1991). In addition, loss of both rapid and slow Ca^{2+} signals delayed the slow RRP recovery process, suggesting that both phasic and tonic Ca^{2+} signals contribute to refilling of the RRP with SVs through an amphiphysin-independent and dynamin 2, 3-dependent endocytic pathway (Lu et al., 2009, Tanifuji et al., 2013). Thus, our findings reveal the existence of novel fast and slow Ca^{2+} transient kinetics that map onto known molecular pathways for endocytosis and RRP maintenance.

Concluding remarks

Molecular Pharmacology Fast Forward. Published on June 30, 2014 as DOI: 10.1124/mol.114.094029
This article has not been copyedited and formatted. The final version may differ from this version.

Collectively, we demonstrated evidence of the time-dependent evolution of Ca^{2+} signals from N-type Ca^{2+} channels following AP firing that regulate exocytosis, RRP replenishment, and short-term plasticity of sympathetic neurons. We propose that, in addition to spatial diffusion of Ca^{2+} (Neher and Sakaba, 2008, Eggermann et al., 2012), time-dependent changes in the concentration of presynaptic Ca^{2+} due to various patterns of AP firing regulate the ability of SVs to respond to incoming signals. Thus, the kinetic organization of phasic and tonic Ca^{2+} signals in and near the AZ may play a role in determining the spatial and molecular aspects of Ca^{2+} regulation of distinct vesicle recycle pathways and pools. Having a diversity of temporal and spatial presynaptic Ca^{2+} signals would allow synapses to dynamically respond to rapid or complex AP bursts, by generating EPSPs that reflect the cell's history of synaptic firing, while simultaneously maintaining the general capability for fast and stable SV recycling and maintenance after single APs.

Molecular Pharmacology Fast Forward. Published on June 30, 2014 as DOI: 10.1124/mol.114.094029
This article has not been copyedited and formatted. The final version may differ from this version.

Acknowledgements

We thank Dr. Charles T. Yokoyama and Dr. Gary J. Stephens for comments on the manuscript.

Author contributions

Participated in research design: Mochida

Conducted experiments: Mori and Tanifuji

Performed data analysis: Mori and Mochida

Wrote or contributed to the writing of the manuscript: Mori and Mochida

Molecular Pharmacology Fast Forward. Published on June 30, 2014 as DOI: 10.1124/mol.114.094029
This article has not been copyedited and formatted. The final version may differ from this version.

Reference

Abbott LF, Regehr WG (2004) Synaptic computation. Nature 431:796-803.

Adler EM, Augustine GJ, Duffy SN, Charlton MP (1991) Alien intracellular calcium chelators attenuate neurotransmitter release at the squid giant synapse. J Neurosci 11:1496-1507.

Angleson JK, Betz WJ (2001) Intraterminal Ca^{2+} and spontaneous transmitter release at the frog neuromuscular junction. J Neurophysiol 85:287-294.

Augustine GJ, Adler EM, Charlton MP (1991) The calcium signal for transmitter secretion from presynaptic nerve terminals. Ann N Y Acad Sci 635:365-381.

Borst JG, Sakmann B (1996) Calcium influx and transmitter release in a fast CNS synapse. Nature 383:431-434.

Catterall WA (2000) Structure and regulation of voltage-gated Ca^{2+} channels. Annual Review of Cell and Developmental Biology 16:521-555.

Catterall WA, Few AP (2008) Calcium Channel Regulation and Presynaptic Plasticity. Neuron 59:882-901.

Catterall WA, Leal K, Nanou E (2013) Calcium channels and short-term synaptic plasticity. J Biol Chem 288:10742-10749.

Cousin MA, Robinson PJ (2001) The dephosphins: dephosphorylation by calcineurin triggers synaptic vesicle endocytosis. Trends Neurosci 24:659-665.

Cummings DD, Wilcox KS, Dichter MA (1996) Calcium-dependent paired-pulse facilitation of miniature EPSC frequency accompanies depression of EPSCs at hippocampal synapses in culture. J Neurosci 16:5312-5323.

Dittman JS, Regehr WG (1998) Calcium dependence and recovery kinetics of presynaptic depression at the climbing fiber to Purkinje cell synapse. J Neurosci 18:6147-6162.

Eggermann E, Bucurenciu I, Goswami SP, Jonas P (2012) Nanodomain coupling between Ca(2)(+) channels and sensors of exocytosis at fast mammalian synapses. Nat Rev Neurosci 13:7-21.

Faas GC, Raghavachari S, Lisman JE, Mody I (2011) Calmodulin as a direct detector of Ca2+ signals. Nature neuroscience 14:301-304.

Hallermann S, Fejtova A, Schmidt H, Weyhersmuller A, Silver RA, Gundelfinger ED, Eilers J (2010) Bassoon speeds vesicle reloading at a central excitatory synapse. Neuron 68:710-723.

Hoppa MB, Lana B, Margas W, Dolphin AC, Ryan TA (2012) alpha2delta expression sets presynaptic calcium channel abundance and release probability. Nature 486:122-125.

Inchauspe CG, Forsythe ID, Uchitel OD (2007) Changes in synaptic transmission properties due to the expression of N-type calcium channels at the calyx of Held synapse of mice lacking P/Q-type calcium channels. J Physiol 584:835-851.

Junge HJ, Rhee J-S, Jahn O, Varoqueaux F, Spiess J, Waxham MN, Rosenmund C, Brose N (2004) Calmodulin and Munc13 Form a Ca^{2+} Sensor/Effector Complex that Controls Short-Term

Synaptic Plasticity. Cell 118:389-401.

Krapivinsky G, Mochida S, Krapivinsky L, Cibulsky SM, Clapham DE (2006) The TRPM7 ion channel functions in cholinergic synaptic vesicles and affects transmitter release. Neuron 52:485-496.

Leao RM, von Gersdorff H (2009) Synaptic vesicle pool size, release probability and synaptic depression are sensitive to Ca^{2+} buffering capacity in the developing rat calyx of Held. Brazilian journal of medical and biological research = Revista brasileira de pesquisas medicas e biologicas / Sociedade Brasileira de Biofisica 42:94-104.

Lee A, Zhou H, Scheuer T, Catterall WA (2003) Molecular determinants of Ca^{2+}/calmodulin-dependent regulation of Cav2.1 channels. Proceedings of the National Academy of Sciences 100:16059-16064.

Libet B, Mochida S (1988) Long-term enhancement (LTE) of postsynaptic potentials following neural conditioning, in mammalian sympathetic ganglia. Brain Research 473:271-282.

Llinás R, Gruner JA, Sugimori M, McGuinness TL, Greengard P (1991) Regulation by synapsin I and Ca^{2+}-calmodulin-dependent protein kinase II of the transmitter release in squid giant synapse. The Journal of Physiology 436:257-282.

Lu W, Ma H, Sheng ZH, Mochida S (2009) Dynamin and activity regulate synaptic vesicle recycling in sympathetic neurons. J Biol Chem 284:1930-1937.

Ma H, Mochida S (2007) A cholinergic model synapse to elucidate protein function at presynaptic terminals. Neurosci Res 57:491-498.

Magupalli VG, Mochida S, Yan J, Jiang X, Westenbroek RE, Nairn AC, Scheuer T, Catterall WA (2013) Ca^{2+}-independent activation of Ca^{2+}/calmodulin-dependent protein kinase II bound to the C-terminal domain of CaV2.1 calcium channels. The Journal of biological chemistry 288:4637-4648.

Mochida S (2011) Ca/Calmodulin and presynaptic short-term plasticity. ISRN Neurol 2011:919043.

Mochida S, Few AP, Scheuer T, Catterall WA (2008) Regulation of presynaptic $Ca_V2.1$ channels by Ca^{2+} sensor proteins mediates short-term synaptic plasticity. Neuron 57:210-216.

Mochida S, Nonomura Y, Kobayashi H (1994) Analysis of the mechanism for acetylcholine release at the synapse formed between rat sympathetic neurons in culture. Microsc Res Tech 29:94-102.

Mochida S, Saisu H, Kobayashi H, Abe T (1995) Impairment of syntaxin by botulinum neurotoxin C1 or antibodies inhibits acetylcholine release but not Ca^{2+} channel activity. Neuroscience 65:905-915.

Mochida S, Sheng ZH, Baker C, Kobayashi H, Catterall WA (1996) Inhibition of neurotransmission by peptides containing the synaptic protein interaction site of N-type Ca^{2+} channels. Neuron 17:781-788.

Mochida S, Westenbroek RE, Yokoyama CT, Itoh K, Catterall WA (2003) Subtype-selective reconstitution of synaptic transmission in sympathetic ganglion neurons by expression of exogenous calcium channels. Proceedings of the National Academy of Sciences of the United

States of America 100:2813-2818.

Nagerl UV, Novo D, Mody I, Vergara JL (2000) Binding kinetics of calbindin-D(28k) determined by flash photolysis of caged Ca^{2+}. Biophys J 79:3009-3018.

Naraghi M (1997) T-jump study of calcium binding kinetics of calcium chelators. Cell Calcium 22:255-268.

Naraghi M, Neher E (1997) Linearized buffered Ca2+ diffusion in microdomains and its implications for calculation of [Ca^{2+}] at the mouth of a calcium channel. J Neurosci 17:6961-6973.

Neher E, Sakaba T (2008) Multiple roles of calcium ions in the regulation of neurotransmitter release. Neuron 59:861-872.

Nicholson-Tomishima K, Ryan TA (2004) Kinetic efficiency of endocytosis at mammalian CNS synapses requires synaptotagmin I. Proc Natl Acad Sci U S A 101:16648-16652.

Poskanzer KE, Marek KW, Sweeney ST, Davis GW (2003) Synaptotagmin I is necessary for compensatory synaptic vesicle endocytosis in vivo. Nature 426:559-563.

Rizzoli SO, Betz WJ (2005) Synaptic vesicle pools. Nat Rev Neurosci 6:57-69.

Sakaba T, Neher E (2001) Calmodulin mediates rapid recruitment of fast-releasing synaptic vesicles at a calyx-type synapse. Neuron 32:1119-1131.

Schneggenburger R, Meyer AC, Neher E (1999) Released fraction and total size of a pool of immediately available transmitter quanta at a calyx synapse. Neuron 23:399-409.

Silver RB, Sugimori M, Lang EJ, Llinas R (1994) Time-Resolved Imaging of Ca^{2+}-Dependent Aequorin Luminescence of Microdomains and QEDs in Synaptic Preterminals. The Biological Bulletin 187:293-299.

Su Susan C, Seo J, Pan Jen Q, Samuels Benjamin A, Rudenko A, Ericsson M, Neve Rachael L, Yue David T, Tsai L-H (2012) Regulation of N-type Voltage-Gated Calcium Channels and Presynaptic Function by Cyclin-Dependent Kinase 5. Neuron 75:675-687.

Takei K, McPherson PS, Schmid SL, De Camilli P (1995) Tubular membrane invaginations coated by dynamin rings are induced by GTP-gamma S in nerve terminals. Nature 374:186-190.

Tanifuji S, Funakoshi-Tago M, Ueda F, Kasahara T, Mochida S (2013) Dynamin isoforms decode action potential firing for synaptic vesicle recycling. J Biol Chem 288:19050-19059.

Thanawala MS, Regehr WG (2013) Presynaptic calcium influx controls neurotransmitter release in part by regulating the effective size of the readily releasable pool. J Neurosci 33:4625-4633.

Tymianski M, Charlton MP, Carlen PL, Tator CH (1994) Properties of neuroprotective cell-permeant Ca^{2+} chelators: effects on [Ca^{2+}]i and glutamate neurotoxicity in vitro. J Neurophysiol 72:1973-1992.

Watanabe S, Rost BR, Camacho-Perez M, Davis MW, Sohl-Kielczynski B, Rosenmund C, Jorgensen EM (2013) Ultrafast endocytosis at mouse hippocampal synapses. Nature 504:242-247.

Wu XS, McNeil BD, Xu J, Fan J, Xue L, Melicoff E, Adachi R, Bai L, Wu LG (2009) Ca^{2+} and calmodulin initiate all forms of endocytosis during depolarization at a nerve terminal. Nat

Neurosci 12:1003-1010.

Yang YM, Fedchyshyn MJ, Grande G, Aitoubah J, Tsang CW, Xie H, Ackerley CA, Trimble WS, Wang LY (2010) Septins regulate developmental switching from microdomain to nanodomain coupling of Ca^{2+} influx to neurotransmitter release at a central synapse. Neuron 67:100-115.

Zucker RS, Regehr WG (2002) Short-term synaptic plasticity. Annu Rev Physiol 64:355-405.

Molecular Pharmacology Fast Forward. Published on June 30, 2014 as DOI: 10.1124/mol.114.094029
This article has not been copyedited and formatted. The final version may differ from this version.

Footnotes: This work was supported by Japan Society of the Promotion of Science, grants-in-aid for Scientific Research B [#25290025] and grants-in-aid for Exploratory Research [#23650169].

Figure Legends

Figure 1. Ca^{2+} chelators reduce SV release probability and availability in the RRP during low frequency firing.

EPSPs were recorded at 0.1 Hz or 0.25 Hz (n=5-8). At time=0, 10-100 μM BAPTA-AM, 1-100 μM EGTA-AM or 0.5% DMSO was bath-applied (A-C, E-G, J-K). EPSP amplitudes were normalized to the averaged amplitudes recorded for 10 min before BAPTA-AM, EGTA-AM or DMSO application. ***A***, ***E***, *a*, Averaged EPSP traces (n=5). *b*, Normalized EPSP traces shown in *a* with expanded time scale. EPSP recordings 5-6 min before and 15-16 min, 25-26 min, 35-36 min after 50 μM BAPTA-AM (***A***) and 1 μM EGTA-AM application (***E***) were averaged and superimposed. ***B***, ***F***, Amplitudes of EPSP recorded at 0.1 Hz were normalized and averaged. The values were smoothed with an 8 point moving average algorithm and plotted against recording time. ***C***, ***G***, Amplitudes of EPSP recorded at 0.1 or 0.25 Hz were normalized and averaged. The values were smoothed with an 8 point moving average algorithm and plotted against recording time. ***D***, ***H***, ***I***, Averaged time constant for the decrease in EPSP amplitudes recorded at 0.1 Hz after the application of 50 or 100 μM BAPTA-AM (*D*), 1-100 μM EGTA-AM (*H*). Comparison of the time constant of EPSP block for 0.1 Hz recording with 0.25 Hz recording C (*I*). Mean ± S.E.M. (n=5-8), *p<0.05, **p<0.03; Bonferroni post hoc test after one-way ANOVA. ***J***, ***K***, EPSP amplitudes recorded at 0.1 Hz were normalized, averaged and plotted against recording time. The values were smoothed with an 8 point moving average algorithm. After the application of 50 μM BAPTA-AM (***J***) or 1 μM EGTA-AM (***K***), EPSP recording was stopped for 20 min. ***L***, Mean reduction of EPSP amplitude measured for 1 min after resuming AP firing. ***M***, ***N***, Postsynaptic ACh response elicited by 100 μM ACh puff-application at 0.1 Hz. 50 μM

BAPTA-AM (M) or 1 μM EGTA-AM (***N***) was applied at time=0. Normalized and averaged ACh responses ± S.E.M (n=4) were plotted against recording time with values smoothed by an 8 point moving average algorithm.

Figure 2. AP-induced Ca^{2+} entry regulates SV availability in the RRP

Changes in EPSP amplitude following an AP-evoked EPSP were monitored by eliciting two consecutive APs at various ISIs from 15 ms to 200 ms, every 1 min, in a presynaptic neuron. Triplicate recordings for each ISI were performed consecutively (n=5), and then 50 μM BAPTA-AM or 1 μM EGTA-AM was bath-applied. 20 min later, another series of paired-EPSP recordings was performed. ***A***, Paired-EPSP traces from one representative recording with ISIs of 15 ms and 120 ms before and after BAPTA application. ***B***, ***C***, Normalized amplitudes of the first and the second EPSPs with BAPTA (***B***) or EGTA (***C***) to that of controls before chelator application were averaged and plotted against various ISIs. ***D***, ***E***, The averaged paired-pulse ratio was plotted against various ISIs. The polynomial fit was expressed as a curved line. Mean ± S.E.M (n=5), *p<0.05, **p<0.01, Mann Whitney U-test.

Figure 3. AP-induced Ca^{2+} entry during high frequency firing regulates SV availability in the RRP

EPSPs evoked by 2-s AP trains at 5 Hz (***A, Ba***), 10 Hz (***A, Bb***), or 20 Hz (***A, Bc***) were recorded every 2 min in triplicate for each frequency, before and 20 min after 50 μM BAPTA-AM, 1 μM EGTA-AM, or 0.5% DMSO bath application (n=5-6). The EPSP amplitude returned to the initial value after 2-min cessation of each AP train, thus, the three EPSP amplitudes are averaged. The reduction of the first EPSP amplitude recorded

Molecular Pharmacology Fast Forward. Published on June 30, 2014 as DOI: 10.1124/mol.114.094029
This article has not been copyedited and formatted. The final version may differ from this version.

at each frequency was 50 ± 3% (5 Hz), 42 ± 5% (10 Hz), and 47 ± 4% (20 Hz) with BAPTA, and 36 ± 3% (5 Hz), 32 ± 6% (10 Hz), 65 ± 8% (20 Hz) with EGTA. ***A***, As a control, 0.5% DMSO showed no effect on synaptic depression. Averaged EPSP amplitude was normalized to the first EPSP amplitude recorded at each frequency. ***B***, Averaged EPSP amplitude from the first to the 10th amplitudes before BAPTA and EGTA applications as a control, and averaged and normalized EPSP amplitudes in the presence of BAPTA or EGTA were superimposed. Mean ± S.E.M. *p<0.05, Mann Whitney U-test *vs*. control. ***C***, Cumulative EPSP amplitudes recorded at 20 Hz were plotted and back-extrapolated to time 0 to estimate RRP size before and after BAPTA (***a***), EGTA (***b***) and DMSO application (***c***).

Figure 4. AP-induced Ca^{2+} entry regulates SV pool recovery

After 1-min control EPSP recordings at 1 Hz, 4-min (***A***-***C***) AP trains at 5 Hz were applied to deplete SVs. The recovery of RRSVs was monitored by measuring EPSP amplitude recorded at 1 Hz (n=4-11). 50 μM BAPTA-AM, 1 μM EGTA-AM, or 0.5% DMSO was bath-applied (***A***-***C***). 19 min, and 39 min later, another series of EPSP recordings were performed. ***A***-***C***, EPSP amplitudes were normalized to the initial mean EPSP amplitudes before the 4-min train. The averaged amplitudes calculated from consecutive EPSP recordings were plotted with smoothed lines using a moving average algorithm. ***D***, ***E***, Single exponential curves fitted to the averaged and normalized EPSP amplitudes 0-2 s (***D***) and 1-6 min (***E***) after cessation of the 5 Hz trains for each series of recordings are shown in ***A***-***C***.

Figure 5. AP-induced Ca^{2+} entry regulates SV availability for short-term plasticities

EPSP amplitude was recorded at 1 Hz. Conditioning stimulus was applied at 0 min. 1 μM EGTA-AM (***A***), 50 μM BAPTA-AM (***B***), or 0.5% DMSO (***C***) was bath-applied at 7 min. 27 min later EPSP recording was resumed and another conditioning stimulus was applied at 29 min. ***A-C***, Averaged EPSP amplitude (n=4-7). 10-s conditioning AP trains at 20 Hz were applied as indicated (arrows). Averaged EPSP amplitudes after the conditioning stimuli were fitted with single exponential decay curve (***A***). (Insert in ***A***) Single exponential decay curves before and after EGTA application were normalized and superimposed. ***D, H,*** Increase in EPSP amplitudes calculated from averaged EPSP amplitudes 1 min before and after conditioning stimulus was expressed as percentage (%). Mean ± S.E.M. *$p<0.05$, Bonferroni post hoc test after one-way ANOVA, EGTA *vs.* BAPTA-AM and DMSO. ***E-G***, Averaged EPSP amplitude (n=6-7). 60-s conditioning AP trains at 40 Hz were applied as indicated (arrows). (Insert in F) EPSP amplitudes after application of the conditioning stimuli were fitted with single exponential decay curve. Single exponential decay curves before and after BAPTA were normalized and superimposed.

Figure 1

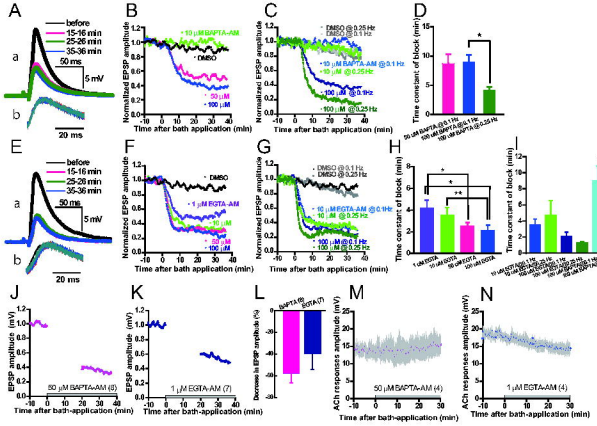
A
before
15-16 min
25-26 min
35-36 min
50 ms
5 mV
a
b
20 ms
B
10 μM BAPTA-AM
DMSO
Normalized EPSP amplitude
Time after bath application (min)
C
DMSO @ 0.33 Hz
DMSO @ 0.1 Hz
10 μM BAPTA-AM @0.1 Hz
10 μM @0.05Hz
100 μM @0.1Hz
100 μM @0.05 Hz
D
Time constant of block (min)
E
F
1 μM EGTA-AM
50 μM
100 μM
G
DMSO @ 0.1 Hz
DMSO @ 0.25 Hz
10 μM EGTA-AM @ 0.1Hz
10 μM @ 0.25 Hz
100 μM @ 0.1 Hz
100 μM @ 0.05 Hz
H
1 μM EGTA
10 μM EGTA
50 μM EGTA
100 μM EGTA
I
J
EPSP amplitude (mV)
50 μM BAPTA-AM (8)
K
1 μM EGTA-AM (7)
L
BAPTA (8)
EGTA (7)
Decrease in EPSP amplitude (%)
M
ACh responses amplitude (mV)
50 μM BAPTA-AM (4)
N
1 μM EGTA-AM (4)

Figure 2

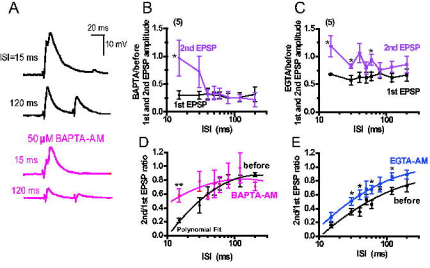
A
20 ms
10 mV
ISI=15 ms
120 ms
50 µM BAPTA-AM
15 ms
120 ms
B
(5)
2nd EPSP
1st EPSP
BAPTA/before
1st and 2nd EPSP amplitude
ISI (ms)
C
(5)
2nd EPSP
1st EPSP
EGTA/before
1st and 2nd EPSP amplitude
ISI (ms)
D
before
BAPTA-AM
Polynomial Fit
2nd/1st EPSP ratio
ISI (ms)
E
EGTA-AM
before
2nd/1st EPSP ratio
ISI (ms)

Figure 3

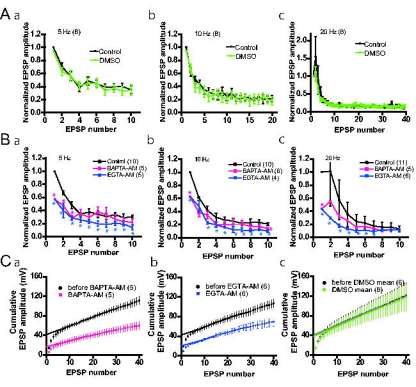
A
a
5 Hz (8)
Control
DMSO
Normalized EPSP amplitude
EPSP number
b
10 Hz (8)
Control
DMSO
Normalized EPSP amplitude
EPSP number
c
20 Hz (8)
Control
DMSO
Normalized EPSP amplitude
EPSP number
B
a
5 Hz
Control (10)
BAPTA-AM (5)
EGTA-AM (5)
Normalized EPSP amplitude
EPSP number
b
10 Hz
Control (10)
BAPTA-AM (6)
EGTA-AM (4)
Normalized EPSP amplitude
EPSP number
c
20 Hz
Control (11)
BAPTA-AM (5)
EGTA-AM (6)
Normalized EPSP amplitude
EPSP number
C
a
before BAPTA-AM (5)
BAPTA-AM (5)
Cumulative EPSP amplitude (mV)
EPSP number
b
before EGTA-AM (6)
EGTA-AM (6)
Cumulative EPSP amplitude (mV)
EPSP number
c
before DMSO mean (6)
DMSO mean (8)
Cumulative EPSP amplitude (mV)
EPSP number

Figure 4

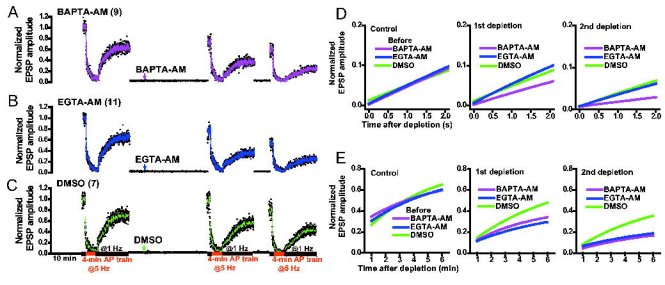
A
BAPTA-AM (9)
BAPTA-AM
B
EGTA-AM (11)
EGTA-AM
C
DMSO (7)
DMSO
Normalized EPSP amplitude
10 min
4-min AP train @5 Hz
@1 Hz
@8 Hz
D
Control
Before
BAPTA-AM
EGTA-AM
DMSO
1st depletion
2nd depletion
Time after depletion (s)
E
Time after depletion (min)

Figure 5

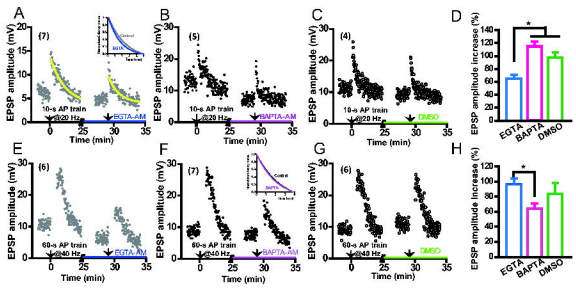
A
B
C
D
E
F
G
H
EPSP amplitude (mV)
Time (min)
10-s AP train
@20 Hz
60-s AP train
@40 Hz
EGTA-AM
BAPTA-AM
DMSO
Control
EGTA
BAPTA
EPSP amplitude increase (%)
EGTA
BAPTA
DMSO
*